A numerical method for a converging cylindrical shock

By R. B. PAYNE
Computing Laboratory, University of Manchester

(*Received* 9 *November* 1956)

SUMMARY

The finite difference method due to Lax (1954) is used to solve the equations of motion for a cylindrically symmetric flow of a compressible fluid. In particular, a converging cylindrical shock is found to increase in strength in agreement with the formula of Chisnell (1957). The artificial diffusion introduced by the method causes the pressure to remain finite at the axis, but a reflected diverging shock is obtained.

1. INTRODUCTION

It is well known that a cylindrical shock wave in a compressible fluid increases in strength as it converges towards the axis. Some spectacular photographs of shocks strengthened in this way have been obtained from experiments performed by Kantrowitz (1951).

The problem when the shock has infinite strength has been successfully solved by Guderley (1942) and Butler (1954), the solution being singular at the axis. For any practical gas there is always some viscosity or heat conduction present which will cause the pressure to remain finite throughout.

Neumann & Richtmyer (1950) have described a finite difference method for calculating compressible fluid flows containing shock waves, a feature of which is the introduction of an artificial diffusion term. In a modification of this method by Lax (1954), the coefficient of the diffusion term is $\Delta x^2/(2\Delta t)$, where Δx is the width of the space mesh and Δt the time interval. Although this is not the correct viscosity or heat conduction term, the effect on the flow will be similar, except in the structure of the diffused shock. In these methods the shock is not regarded as an interior boundary, but appears as a steep gradient of the variables over a few mesh points. The amount of diffusion introduced is very large, as may be seen by considering the width of the shock. For air at 300° K, the width is of the order of a few mean paths; so that if the flow in one-thousandth of a centimetre of air is considered (this distance being covered by 100 mesh points, which entails a reasonable length of calculation), the amount of diffusion introduced is comparable with what it would be for real viscosity and heat conduction.

In this paper, calculations by Lax's method of flows involving converging cylindrical shocks are described. It is necessary to give special consideration to the flow at the axis, and a reflected diverging shock is obtained in each case. The pressure at the axis remains finite due to the diffusion introduced.

The converging shock is started by taking initial conditions as in a shock tube, namely by considering a cylindrical diaphragm separating two uniform regions of a gas at rest with a higher pressure in the outside region, the flow being started by the rupture of the diaphragm. Let the ratios of the pressures and densities on the two sides of the diaphragm be p^* and $\rho^*(p^* > 1)$. In a shock tube, if $p^* = \rho^*$ (that is, the uniform temperature on the two sides is the same), a shock travels into the low-pressure region followed by a contact surface, and an expansion fan travels into the high-pressure region. By a suitable choice of p^* and ρ^*, it is possible to obtain a shock wave and expansion fan with no contact surface.

In this way a converging cylindrical shock of strength 2 is obtained (the strength of a shock is defined as the pressure ratio across it). It is found that the contact surface does not affect the converging shock, which behaves identically for the flow without a contact surface. When stronger shocks are considered, the inaccuracy of the method in the vicinity of the contact surface is apparent, and it becomes necessary to eliminate the contact surface by having the gas outside the cylindrical diaphragm initially at a higher temperature than that inside. For a shock of initial strength 8, it is found that the inaccuracy of the calculations for the part of the flow occupied by the expansion fan also affects the region of the converging shock.

In each case the calculations were performed with a set of mesh points uniformly spaced from the axis to twice the radius of the cylindrical diaphragm. The mesh width is taken as 1/64 of the radius. For 140 time steps of the integration over these 128 points, the time taken on the Manchester University Mark I electronic digital computer was 5 hours. (This included the repetition of each step to provide a check by the consistency of the computer.) Each calculation was repeated with a coarser mesh of twice this width. One calculation was also performed with half this mesh width, taking 16 hours of computing time. The width of the shock is proportional to the mesh width.

The strength of the converging shock is found to be in good agreement with the formula given by Chisnell (1957). Near the axis the strength falls below his predicted value. The amount of entropy left behind the outgoing shock is also calculated.

2. Method

2.1. *Differential equations of motion*

The cylindrically symmetric flow of an inviscid compressible gas with constant specific heats and without heat conduction satisfies the following equations:

$$\frac{\partial}{\partial t}(r\rho) + \frac{\partial}{\partial r}(r\rho u) = 0, \tag{1a}$$

$$\frac{\partial}{\partial t}(r\rho u) + \frac{\partial}{\partial r}(r\rho u^2) + r\frac{\partial p}{\partial r} = 0, \tag{1b}$$

$$\frac{\partial}{\partial t}(rE) + \frac{\partial}{\partial r}(rEu + rpu) = 0, \tag{1c}$$

in which r is the distance from the axis, t the time, u the velocity, ρ the density, p the pressure, and E is the sum of the internal energy and kinetic energy per unit volume: i.e.

$$E = \frac{p}{\gamma - 1} + \tfrac{1}{2}\rho u^2,$$

where γ is the ratio of the specific heats.

Equations (1) may be made non-dimensional by putting

$r = r_0 r'$, where r_0, a constant, is the radius of the diaphragm;
$\rho = \rho_0 \rho'$, where ρ_0 is the initial density of the gas inside the diaphragm;
$p = p_0 p'$, where p_0 is the initial pressure of the gas inside the diaphragm;
$u = u_0 u'$, where $u_0 = (\gamma p_0/\rho_0)^{1/2}$ is the velocity of sound in the gas inside the diaphragm;
$t = t_0 t'$, where $t_0 = r_0/u_0$;
$E = p_0 E'$.

This gives

$$\frac{\partial}{\partial t'}(r'\rho') + \frac{\partial}{\partial r'}(r'\rho'u') = 0, \tag{2a}$$

$$\frac{\partial}{\partial t'}(r'\rho'u') + \frac{\partial}{\partial r'}(r'\rho'u'^2) + \gamma^{-1/2} r' \frac{\partial p'}{r'} = 0, \tag{2b}$$

$$\frac{\partial}{\partial t'}(r'E') + \frac{\partial}{\partial r'}(r'E'u' + r'p'u') = 0, \tag{2c}$$

where

$$E' = \frac{p'}{\gamma - 1} + \frac{\gamma}{2}\rho' u'^2.$$

Hereafter these non-dimensional variables will be used and the primes will be omitted.

It is convenient to introduce new variables $a = r\rho$, $b = r\rho u$, $c = rE$. The equations of motion then become

$$\frac{\partial a}{\partial t} + \frac{\partial b}{\partial r} = 0, \tag{3a}$$

$$\frac{\partial b}{\partial t} + \frac{\partial}{\partial r}(bu) + \gamma^{-1/2} r \frac{\partial p}{\partial r} = 0, \tag{3b}$$

$$\frac{\partial c}{\partial t} + \frac{\partial}{\partial r}(cu + rpu) = 0, \tag{3c}$$

where

$$\rho = \frac{a}{r}, \tag{4a}$$

$$u = \frac{a}{b}, \tag{4b}$$

$$p = \frac{(\gamma - 1)c}{r} - \frac{\gamma(\gamma - 1)}{2} bu. \tag{4c}$$

2.2. *Finite difference equations*

Consider a set of mesh points $r = k\Delta r$, $t = t_n$, where k and n are non-negative integers and where Δr is a constant such that $K = (\Delta r)^{-1}$ is an integer. Let $t_{n+1} - t_n = \Delta t_n$, and let $\phi_{k,n}$ denote $\phi(r, t)$, where $r = r_k = k\Delta r$ and $t = t_n$.

Let us postpone discussion of the fact that equation (3 b) is not in the 'conservation form' desired by Lax (see § 2.3), and, otherwise following him, replace derivatives by differences as follows. At the point $r = r_k$, $t = t_n$, replace

$$\frac{\partial \phi}{\partial t} \quad \text{by} \quad \frac{\phi_{k,n+1} - \frac{1}{2}(\phi_{k+1,n} + \phi_{k-1,n})}{\Delta t_n}, \tag{5 a}$$

and

$$\frac{\partial \phi}{\partial r} \quad \text{by} \quad \frac{\phi_{k+1,n} - \phi_{k-1,n}}{2\Delta r} \tag{5 b}$$

We hence obtain explicit equations for the values of the variables a, b, c at time t_{n+1} in terms of the variables at time t_n, namely

$$a_{k,n+1} = \tfrac{1}{2}(a_{k-1,n} + a_{k+1,n}) + \frac{\Delta t_n}{2\Delta r}(b_{k-1,n} - b_{k+1,n}), \tag{6 a}$$

$$b_{k,n+1} = \tfrac{1}{2}(b_{k-1,n} + b_{k+1,n}) + \frac{\Delta t_n}{2\Delta r}\{b_{k-1,n}\, u_{k-1,n} - b_{k+1,n}\, u_{k+1,n} + \gamma^{-1/2} r_k (p_{k-1,n} - p_{k+1,n})\}, \tag{6 b}$$

$$c_{k,n+1} = \tfrac{1}{2}(c_{k-1,n} + c_{k+1,n}) + \frac{\Delta t_n}{2\Delta r}(c_{k-1,n}\, u_{k-1,n} - c_{k+1,n}\, u_{k+1,n} + r_{k-1}\, p_{k-1,n}\, u_{k-1,n} - r_{k+1}\, p_{k+1,n}\, u_{k+1,n}). \tag{6 c}$$

From these equations the values of u, ρ and p are obtained by equations (4). It may be remarked that (i) equations (6) do not apply for $k = 0$, and (ii) the values of variables at points on the two staggered lattices, $k+n$ even and $k+n$ odd, are independent of each other.

2.3. *The pressure term*

As remarked above, the pressure term $\gamma^{-1/2} r\, \partial p/\partial r$ in the momentum equation (3 b) is not the derivative of a function of r as is desired for Lax's method. The effect of the pressure is clearer when the difference equations are derived from the conditions of conservation of mass, momentum and energy in the space

$$(k-1)\Delta r \leqslant r \leqslant (k+1)\Delta r,$$
$$0 \leqslant \theta \leqslant \epsilon,$$

where θ is the azimuthal angle and $\epsilon \ll 1$. In the momentum equation, the terms involving the pressure are

$$\frac{\Delta t_n}{2\Delta r}\gamma^{-1/2}\left(r_{k-1}\, p_{k-1,n} - r_{k+1}\, p_{k+1,n} + \int_{(k-1)\Delta r}^{(k+1)\Delta r} p\, dr\right).$$

Possible approximations for $\int p\, dr$ are

$$(p_{k-1,n} + p_{k+1,n})\Delta r, \tag{7 a}$$

$$2p_{k,n}\Delta r, \tag{7 b}$$

$$\tfrac{1}{3}(p_{k-1,n} + 4p_{k,n} + p_{k+1,n})\Delta r. \tag{7 c}$$

The calculation of a particular flow was done using each of these three approximations in turn, and the solutions after 60 time steps were compared. It was found that away from the shock the differences between the solutions

were negligible, and even at the shock the results for u, ρ and p differed by less than 1%. In view of this, the approximation (7 a), which has the advantage that the two staggered lattices are independent, was chosen.

2.4. *The flow at the axis*

At the axis ($k = r = 0$), we have $u = 0$ and also $a = r\rho = 0$, $b = r\rho u = 0$, $c = rE = 0$. To obtain the density and pressure it is necessary to resort to an approximation different from (6). Several formulae for the density and pressure were deduced, and many of these were used in trial calculations.

The conservation of mass in a cylinder of radius Δr may be written

$$\frac{\partial}{\partial t}\left\{\int_{r=0}^{r=\Delta r} \rho(r,t)\, d(r^2)\right\} + 2\,\Delta r \rho(\Delta r, t) u(\Delta r, t) = 0.$$

Taking the approximation $\frac{1}{2}\{\rho(0,t)+\rho(\Delta r,t)\}\Delta r^2$ for this integral, and by similarly considering a cylinder of radius $2\Delta r$, we obtain

$$\rho_{0,n+1} = \rho_{1,n} + \frac{\Delta t_n}{\Delta r}(\tfrac{1}{4}\rho_{3,n} u_{3,n} - \tfrac{11}{4}\rho_{1,n} u_{1,n}). \tag{8 a}$$

From consideration of conservation of energy we similarly obtain

$$E_{0,n+1} = E_{1,n} + \frac{\Delta t_n}{\Delta r}(\tfrac{1}{4}E_{3,n} u_{3,n} + \tfrac{1}{4} p_{3,n} u_{3,n} - \tfrac{11}{4}E_{1,n} u_{1,n} - \tfrac{11}{4} p_{1,n} u_{1,n}), \tag{8 b}$$

whence

$$p_{0,n+1} = (\gamma - 1)E_{0,n+1}.$$

In common with equations (6), equations (8) use a staggered mesh.

When trial calculations were made, it was found that in the pressure and density at the axis, oscillations developed and rapidly increased in amplitude. (The oscillations for the two independent staggered lattices usually differed in phase and amplitude.) It was found that this numerical instability appeared to be eliminated by using the approximation (7 c) at the point $k = 1$. Thus, for $k = 1$, equation (6 b) is replaced by

$$b_{1,n+1} = \tfrac{1}{2} b_{2,n} + \frac{\Delta t_n}{2\Delta r}\{-b_{2,n} u_{2,n} + \gamma^{-1/2}\Delta r(\tfrac{1}{3} p_{0,n} + \tfrac{4}{3} p_{1,n} - \tfrac{5}{3} p_{2,n})\}. \tag{9}$$

In all calculations done with this modification to equations (6), oscillations at the axis did not appear. However, the term in $p_{1,n}$ makes the two staggered lattices no longer independent of each other.

2.5. *Initial conditions*

To calculate the flow near the axis it was found necessary to perform the integration simultaneously for the two staggered lattices. (That is, the calculation is performed at all the points $k = 0, 1, 2...$ at each step in time $n = 0, 1, 2...$.) This adds importance to the precise initial values of the variables in the neighbourhood of the diaphragm. At the diaphragm $k = K$, the variables are chosen so that $a_{K,0}$, $b_{K,0}$, $c_{K,0}$ are the respective averages for

$k = K \pm 1$ of $a_{k,0}$, $b_{k,0}$, $c_{k,0}$. Thus the initial conditions are taken as

$$u_{k,0} = 0, \quad \text{for all } k,$$

$$\rho_{k,0} = 1,\ p_{k,0} = 1, \quad \text{for } k<K,$$

$$\left.\begin{aligned} \rho_{K,0} &= \tfrac{1}{2}(\rho^* + 1) + \frac{\Delta r}{2}(\rho^* - 1), \\ p_{K,0} &= \tfrac{1}{2}(p^* + 1) + \frac{\Delta r}{2}(p^* - 1), \end{aligned}\right\}$$

$$\rho_{k,0} = \rho^*,\ p_{k,0} = p^*, \quad \text{for } k<K,$$

where ρ^* and p^* are constants.

2.6. *The time interval*

In his paper Lax mentioned the Courant–Friedrichs–Lewy criterion as a necessary condition for the stability of this numerical method. In this problem the largest velocity is that of the shock, so that this necessary condition for stability is

$$\Delta t_n/\Delta r \leqslant 1/(\text{velocity of shock wave}).$$

Also, the width of the shock depends on the value of $\Delta t_n/\Delta r$, and is smallest when this is as large as possible.

A series of trial calculations were made choosing Δt_n so that

$$\Delta t_n/\Delta r = A/(\text{velocity of shock wave}),$$

where A assumed various constant values. For a weak shock the method of calculation was unstable with $A = 0{\cdot}9$, but with $A \leqslant 0{\cdot}85$ it appeared to be stable. (Any instability first showed at the rear of the shock.) Hence the time interval was chosen as above with $A = 0{\cdot}85$. For stronger shock waves this choice of time interval also gave instability, and for the strongest shock (initial strength 8) it was found necessary to further reduce the time interval by taking $A = 0{\cdot}75$.

Throughout, the time interval was chosen for the next step from the shock velocity in the previous step, which does not involve any iteration. This shock velocity was calculated from the distance moved by the shock, the position of the shock ($r = R$) being determined from the pressure distribution. This was done by linearly interpolating in the table of $p_{k,n}$ against r_k to find the point where p is the average of the pressures behind and in front of the shock. The pressure behind the shock is taken as the local maximum value of $p_{k,n}$. For the shock converging towards the axis, the pressure in front of the shock was taken as $p_{0,n}$, the pressure at the axis. For the diverging shock, the pressure in front of the shock was defined as the pressure at the point where $p(r-\Delta r, t_n) - p(r, t_n) = B$, where suitable values for the constant B were found to be: 0·1 for a weak shock of strength 2 initially; 0·2 for a shock of initial strength 4; 0·4 for a strong shock of strength 8 initially.

When near the axis, the position of the shock is not identified sufficiently accurately. The procedure adopted was to keep the time interval constant at the value it has obtained as the axis is approached. When Δt_n was kept at this small value, the reflected shock was so diffused that it was impossible

to recognize it. The outgoing shock travels at a lower velocity, thus permitting a larger time interval. Therefore, after a few steps, a larger constant time interval $\Delta t_n = C$ was taken. The value of C was chosen so that when it was possible to adjust the time interval from the velocity of the outgoing shock, the value of Δt_n was then slightly greater than C.

This method of adjusting Δt_n was found to be sufficient to prevent the appearance of numerical instability due to the use of too large a time interval, and to avoid excessive spreading of the shock due to taking Δt_n much smaller than the permissible maximum.

3.1. *Initial pressure and density ratio* 4

For a shock tube, the initial conditions specified by $p^* = \rho^* = 4$ give a shock of strength 1·93, a contact surface and an expansion fan. The solution is obtained for a cylindrical diaphragm with these initial conditions,

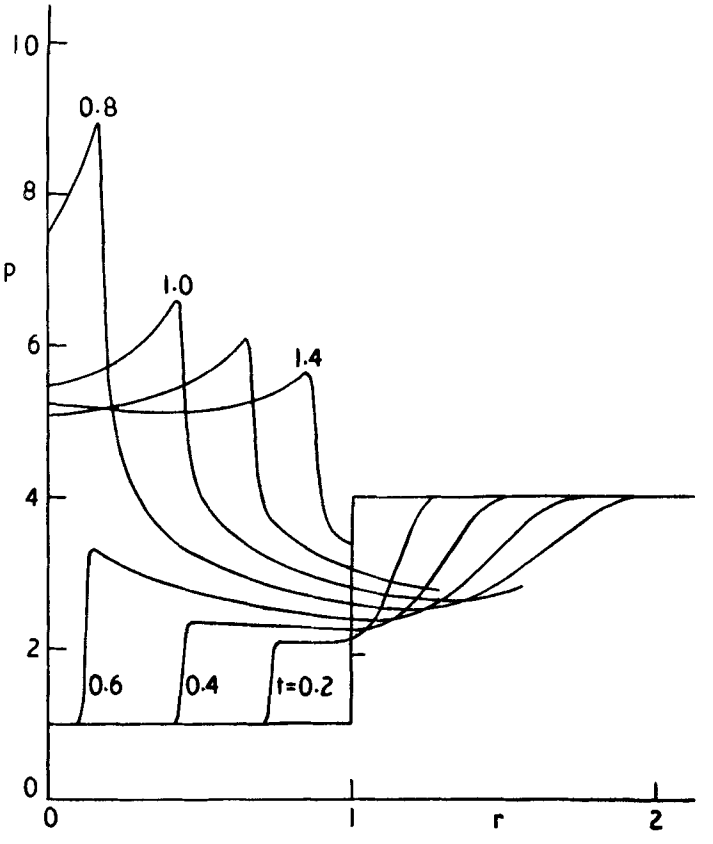

Figure 1. Pressure *vs* radius at intervals 0·2 of time for a flow initiated by a cylindrical diaphragm with initial pressure and density ratios 4. The converging shock of initial strength 1·93 increases in strength and reaches the axis at $t = 0{\cdot}66$, and a reflected shock is obtained. An expansion fan travels out from the diaphragm. The width of the space mesh used is 0·008 units where the radius of the diaphragm is 1 unit, the pressure ahead of the converging shock being the unit of pressure.

a converging cylindrical shock initially of strength 1·93 being obtained. The mesh width $\Delta r = 1/128$ is used.

In figure 1 the pressure distribution is shown at intervals 0·2 of time (each representing about 40 steps of the integration). Apart from the first few steps of the integration, the shock appears as a rapid variation in p over about six points of the space mesh. As t increases and the shock

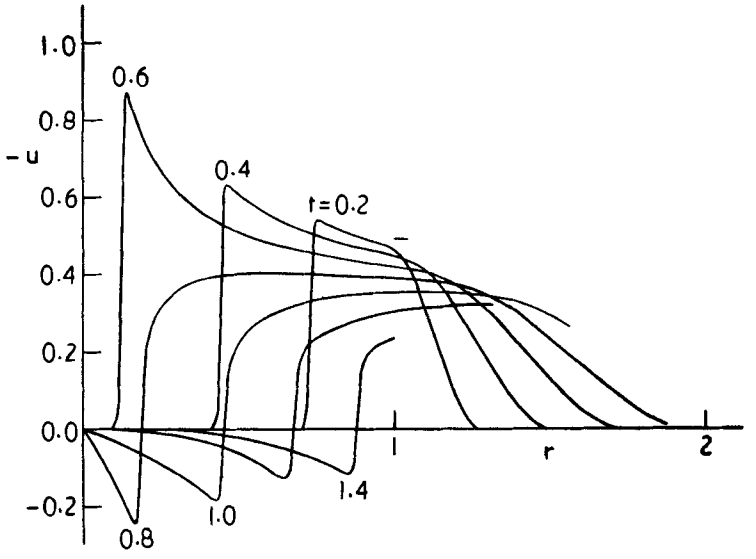

Figure 2. Velocity *vs* radius at intervals 0·2 of time for a flow initiated by a cylindrical diaphragm with initial pressure and density ratios 4. The unit of velocity is the velocity of sound in the undisturbed gas ahead of the converging shock.

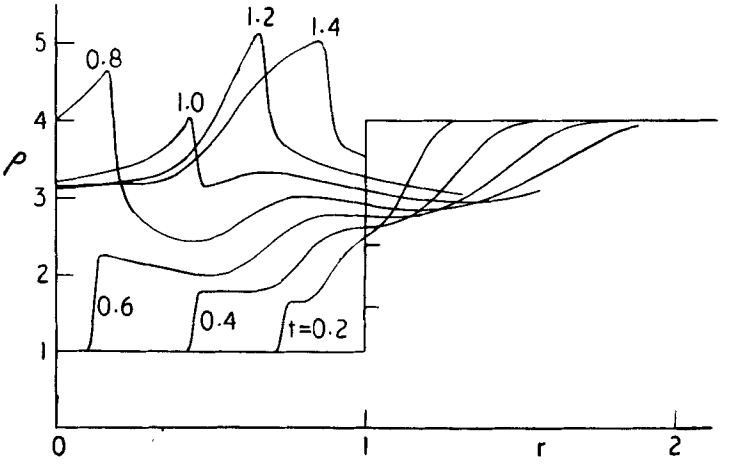

Figure 3. Density *vs* radius at intervals 0·2 of time for a flow initiated by a cylindrical diaphragm with initial pressure and density ratios 4. The contact surface is spread over a large number of mesh points. The density is unity ahead of the converging shock.

moves in towards the axis, the strength of the shock is seen to increase. After the shock has passed, the pressure at any fixed point behind it continues to rise. When the shock reaches the axis, the pressure there rises to a high but finite value (figure 5), and a reflected diverging shock appears. The pressure at a fixed point behind the reflected shock decreases as t increases.

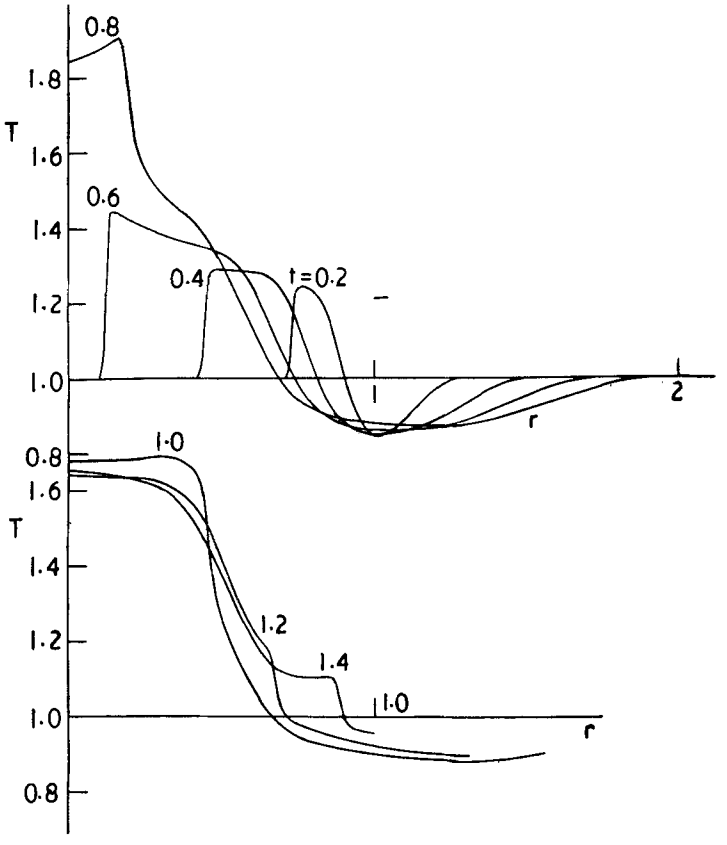

Figure 4. Temperature *vs* radius at intervals 0·2 of time for a flow initiated by a cylindrical diaphragm with initial pressure and density ratios 4. The diverging shock leaves a region of heated gas between the axis and the contact surface. The initial temperature of the gas is unity.

In figure 2 the velocity of the gas in this flow is seen to behave similarly, except of course that the converging shock decreases the gas velocity from zero to a negative (inwards) value. The diverging shock increases the gas velocity to a small positive (outwards) value. Behind the converging shock, the velocity at a fixed point also increases with time and decreases when the diverging shock has passed.

The graphs of the density (figure 3) are similar to those of the pressure, but the rise in density across the shock is smaller, corresponding to a temperature increase. In the distributions of both density and temperature

(figure 4), the contact surface appears. Unlike the shock, this is far from being a discontinuity in these variables; it is a gradual change spread over an increasing number of mesh points. The contact surface moves inwards behind the converging shock, and is traversed by the diverging shock. At $t = 1{\cdot}4$, the shock has more or less passed the smudged contact surface, leaving a region of high temperature between the axis and contact surface (see § 3.5).

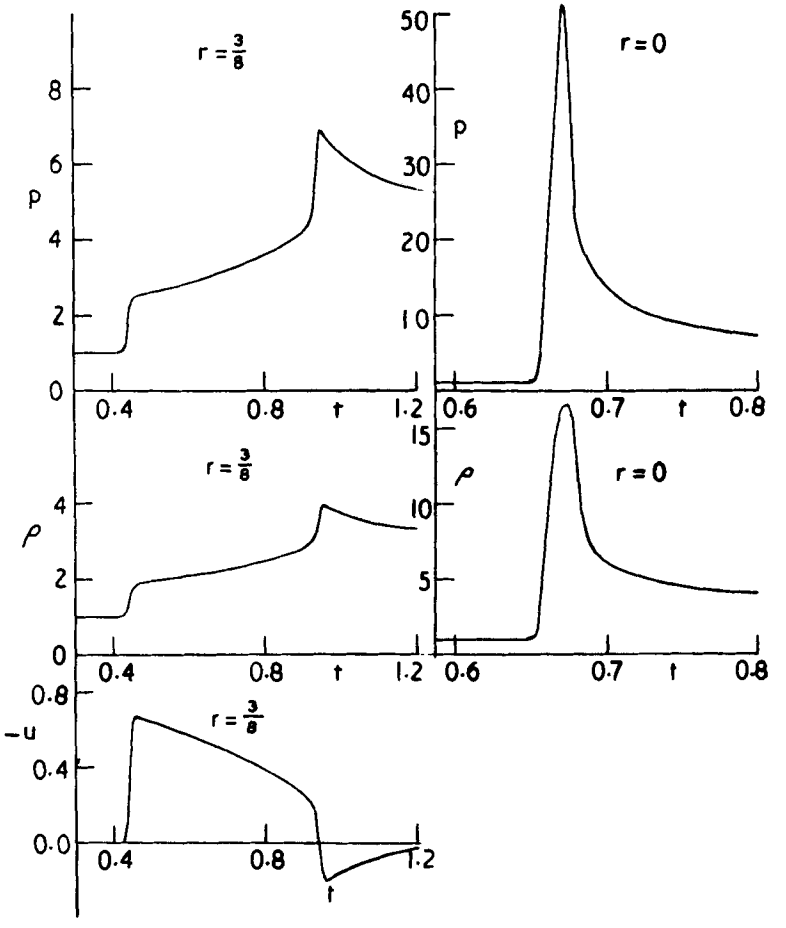

Figure 5. Pressure, density and velocity *vs* time at the fixed point $r = 0{\cdot}375$. At the axis $r = 0$, the two rapid changes in p and ρ when the converging and diverging shocks pass are merged. The velocity is zero at the axis.

The variation with time of the variables at fixed points $r = 0$ and $r = 0{\cdot}375$ is shown in figure 5. Although the general features resemble the solution given by Guderley (1942), the magnitudes of the variables are considerably smaller since the condition of infinite shock strength is not fulfilled.

3.2. *Stronger shock: heated external region*

With the above initial conditions ($p^* = \rho^*$), a contact surface is produced which cannot be satisfactorily treated by this method of Lax (1954). With the shock wave, where the density, velocity and pressure decrease in the direction of motion, there is the tendency of the flow to make the wave narrower, which balances the spreading effect of diffusion. With a contact surface, there is no such balancing effect and diffusion continues unimpeded. When a higher pressure ratio was used, the spreading of the contact surface increased and appreciably affected the shock. In order to eliminate the undesirable contact surface, values of p^* and ρ^* were chosen such that the shock-tube equations are satisfied with a contact surface of zero strength. For example, the values $p^* = 3{\cdot}52$, $\rho^* = 2{\cdot}44$ satisfy the shock-tube equation with no contact surface and a shock of strength 1·93 (which is the same strength as that given by $p^* = \rho^* = 4$). With these initial conditions, the converging cylindrical shock behaves identically. Differences in the diverging shock only occur when in the former case ($p^* = \rho^* = 4$) the contact surface is traversed. On passing into a colder region, the shock travels more slowly. Similarly, the outgoing expansion fan travels more quickly in the latter case when the external region is at a higher temperature.

By initially heating the external region to eliminate the contact surface, it is possible to obtain a stronger converging shock, and results were obtained for flows with shocks of initial strengths 4 and 8. A mesh width $\Delta r = 1/64$ was used. The distributions of pressure, velocity, density and temperature at intervals 0·1 of time are shown for the latter example in figures 6 to 9. The general features of the behaviour of the variables are the same as for the weak shock (strength 1·93 initially). As predicted by Chisnell (see § 3.3), the stronger shock increases in strength more rapidly than the weak shock as it approaches the axis.

From the pressure distributions (or perhaps more clearly from the velocity distributions), it will be seen that for the stronger shock flow the expansion fan has increased diffusion. (This is partly but not entirely due to the use of a coarser space mesh.) This diffusion is particularly noticeable in the first few steps of the integration. It is not unreasonable to suspect that the diffusion from the expansion fan may affect the converging shock.

3.3. *Strength of converging shock*

The position and strength of the shock at any instant of time are deduced from the pressure *vs* radius distributions such as are shown in figures 1 and 6 (see § 2.6). The strength of the shock is taken as the maximum value of the pressure in the p/r distributions. Because of the spreading of the shock over several mesh points, the strength of the shock will be underestimated when the axis is approached, and the position of the shock is also possibly in error by the order of one mesh length.

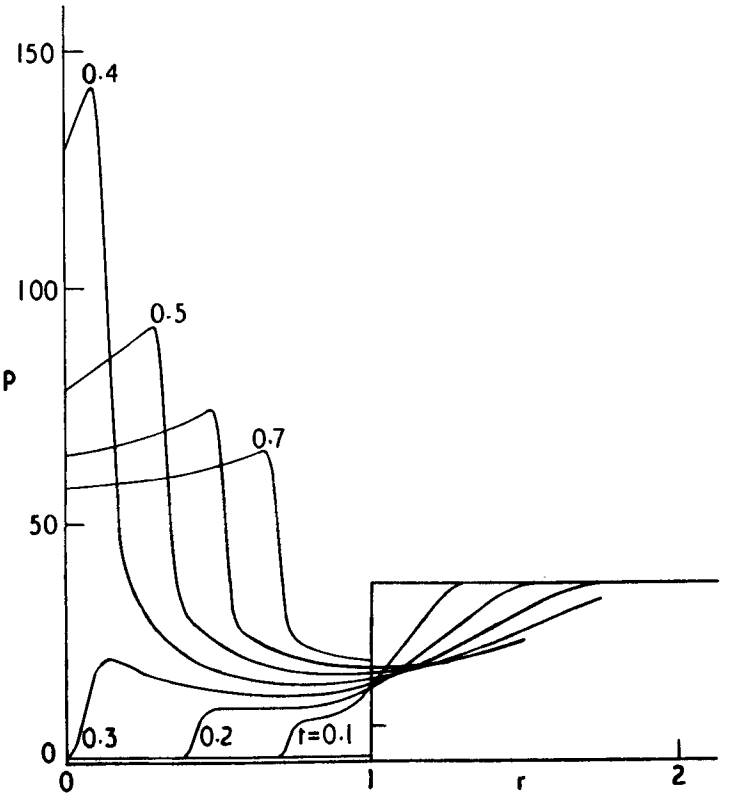

Figure 6. Pressure *vs* radius at intervals 0·1 of time for a flow initiated by a cylindrical diaphragm with initial pressure ratio 38·2 and density ratio 10·7. The converging shock begins at strength 8 and reaches the axis at $t = 0{\cdot}31$. Much greater rises in pressure are obtained with this stronger shock. The width of the space mesh is 0·016 and the pressure ahead of the shock is unity.

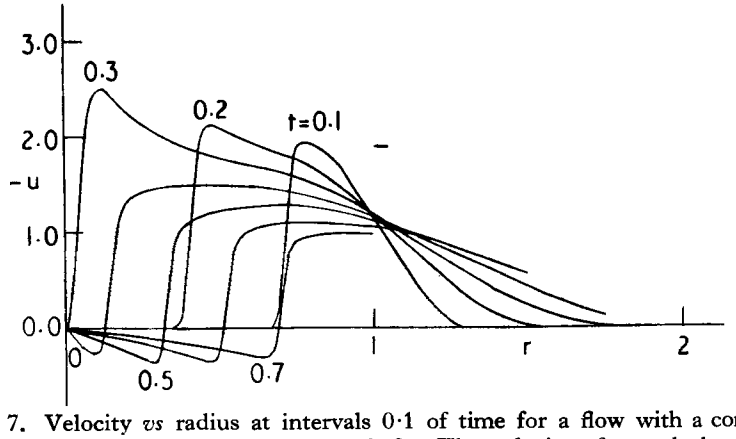

Figure 7. Velocity *vs* radius at intervals 0·1 of time for a flow with a converging cylindrical shock of initial strength 8. The velocity of sound ahead of the converging shock is unity.

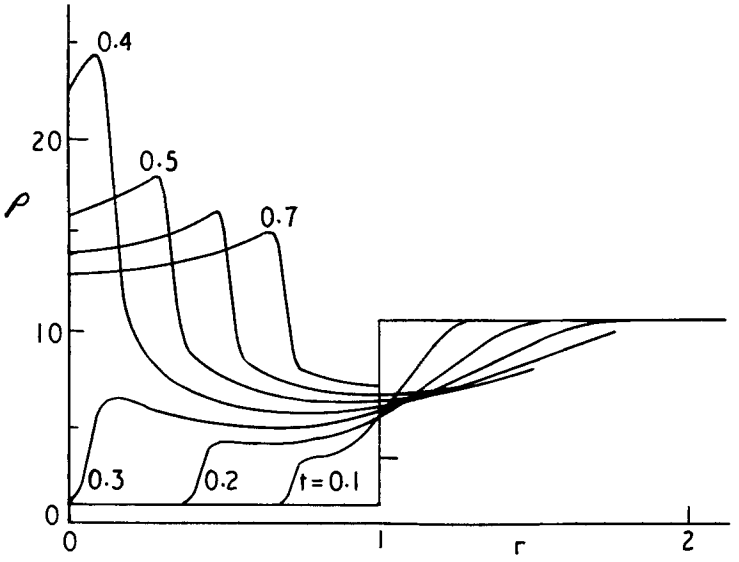

Figure 8. Density *vs* radius at intervals 0·1 of time for a flow with a converging cylindrical shock of initial strength 8. The density ahead of the converging shock is unity.

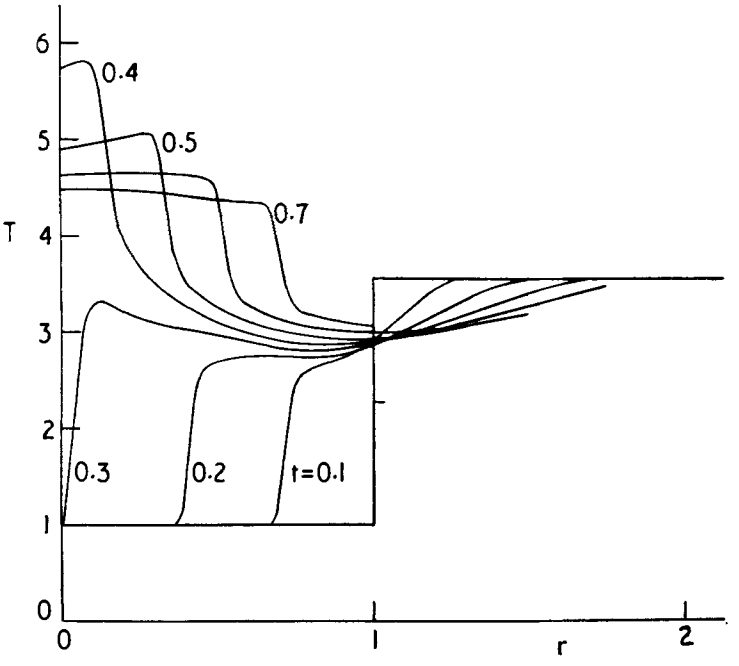

Figure 9. Temperature *vs* radius at intervals 0·1 of time for a flow with a converging cylindrical shock of initial strength 8. Initially the temperature between the axis and diaphragm is unity, and beyond the diaphragm is 3·57.

In view of the crudeness of this part of the calculation, it is perhaps remarkable that the results obtained should fit a smooth curve of z *vs* R, where z is the shock strength and R is the radius of the shock (figures 10, 11). The agreement with the formula (obtained by Chisnell (1957)) for the strength of a converging cylindrical shock is extremely good. The divergence from his predicted strength only appears near the axis and decreases with the mesh width.

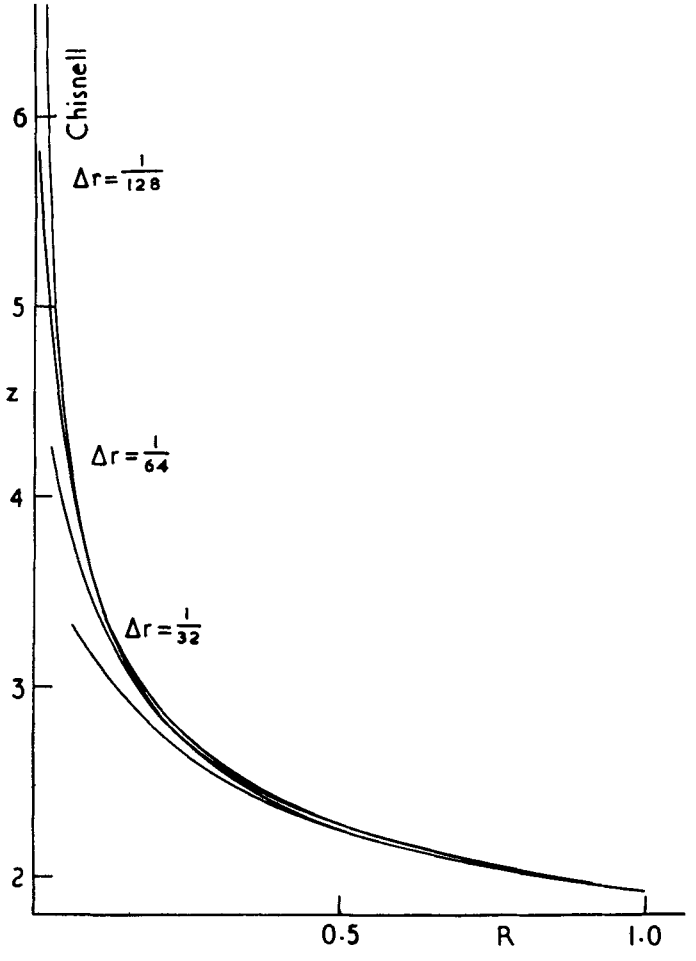

Figure 10. Shock strength *vs* radius for a converging cylindrical shock of initial strength 1·93. The agreement with Chisnell's formula is better when a finer mesh is used.

For a stronger shock the agreement is not so outstandingly good. The strength obtained is greater than Chisnell's. This deviation is attributed to the effect of diffusion from the expansion fan (see § 3.2).

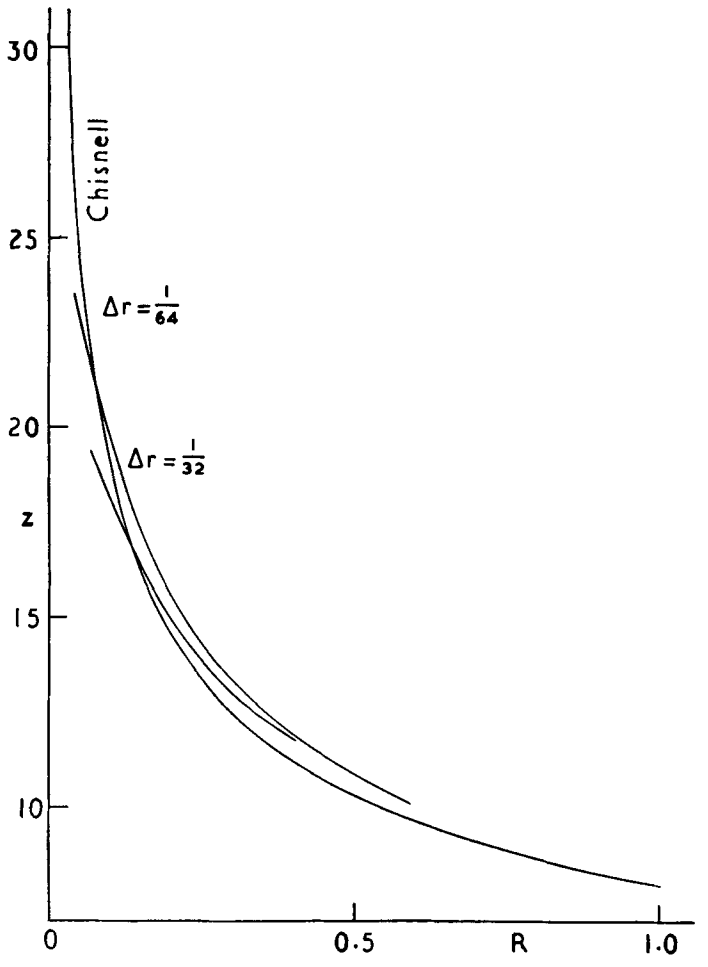

Figure 11. Shock strength *vs* radius for a converging cylindrical shock of initial strength 8. Errors arise from the diffusion of the expansion fan.

3.4. *Variation of gas constant* γ

The results described above are for a gas with $\gamma = 7/5$. The calculations were repeated for the flow with initial conditions specified by $p^* = \rho^* = 4$, with $\gamma = 5/3$. The pressure distributions were very similar to the former flow, the initial shock being just slightly weaker. The variation of shock strength with distance from the axis was again in good agreement with Chisnell's theory. A larger density change across the contact surface was obtained. The temperature near the axis when the diverging shock had traversed the contact surface was much higher, being 1·95. The larger temperature variation was accompanied by a smaller gas velocity.

3.5. *Entropy increase due to cylindrical shock*

When the reflected diverging shock has travelled out, a region of gas at high temperature and almost at rest is left between the axis and the contact

surface (figures 2 and 4). The high temperature indicates that a considerable amount of energy has been dissipated by the shock. For a perfect gas without any diffusion, the flow is isentropic except on passing through the shock. There is no change in the entropy per unit mass in flow through the expansion fan, and there is no flow through the contact surface, at which, however, there is a discontinuity in entropy. Hence, when the diverging shock has passed, the total entropy of the gas between the axis and the contact surface will be constant (assuming no subsequent shocks pass through this region). This heated gas is the gas which was initially between the axis and the diaphragm, the shock having passed through it on both its inward and outward journeys.

The entropy increase produced by the shock is calculated as follows. The contact surface $r = \alpha$ is located by the fact that the mass of gas between the axis and contact surface is constant, that is, by finding α such that

$$\int_0^\alpha 2\pi\rho r\,dr = \int_0^1 2\pi r\,dr = \pi.$$

The total entropy per unit length in this gas is

$$\int_0^\alpha 2\pi c_v(\log p - \gamma \log \rho)\rho r\,dr,$$

where c_v is the specific heat at constant volume. The integrals were evaluated by Simpson's rule, and, for the flow with initial conditions specified by $p^* = \rho^* = 4$, gave large negative values for this entropy which also decrease with time. The initial entropy of this gas is zero, and the entropy per unit mass behind the initial shock is $0{\cdot}011c_v$ and is greater for stronger shocks. However, the entropy per unit mass in the gas initially outside the diaphragm is $-0{\cdot}555c_v$, and diffusion of entropy across the contact surface exceeds the production of entropy by the shock.

For the flow with the same initial shock strength but with the gas initially heated to give a contact surface of zero strength, the entropy per unit mass outside the diaphragm is $0{\cdot}011c_v$ which is the same as the entropy behind the initial shock. Diffusion across the contact surface will be reduced, making this a more suitable flow from which to calculate the entropy produced by the shock. The total entropy per unit length left between the axis and contact surface is found to be $0{\cdot}077c_v$. This may be compared with a plane shock of strength 1·93 reflected normally by a plane solid wall. The increase in the total entropy in a mass π of gas is $0{\cdot}063c_v$ for a plane shock reflection.

References

Butler, D. S. 1954 *Armaments Research Establishment Rep.* no. 54/55.

Chisnell, R. F. 1957 *J. Fluid Mech.* **2** (in the press).

Guderley, G. 1942 *Luftfarhtforschung* **19**, 302–312.

Kantrowitz, A. & Perry, R. W. 1951 *J. Appl. Phys.* **22**, 878–886.

Lax, P. D. 1954 *Comm. Pure Appl. Math.* **7**, 159–193.

Neumann, J. von & Richtmyer, R. D. 1950 *J. Appl. Phys.* **21**, 232–237.